Optical Analysis and Reappraisal of the Peripheral Light Focusing Theory of Nasal Pterygia Formation

P. Ewen King-Smith,[1] Thomas F. Mauger,[2] Carolyn G. Begley,[3] and Patrice Tankam[3]

[1]The College of Optometry, Ohio State University, Columbus, Ohio, United States
[2]West Virginia University Eye Institute, Morgantown, West Virginia, United States
[3]School of Optometry, Indiana University, Bloomington, Indiana, United States

Correspondence: P. Ewen King-Smith, College of Optometry, The Ohio State University, 338 W 10th Avenue, Columbus, OH 43210-1280, USA; king-smith.1@osu.edu.

Received: July 10, 2019
Accepted: December 10, 2019
Published: February 27, 2020

Citation: King-Smith PE, Mauger TF, Begley CG, Tankam P. Optical analysis and reappraisal of the peripheral light focusing theory of nasal pterygia formation. *Invest Ophthalmol Vis Sci.* 2020;61(2):42. https://doi.org/10.1167/iovs.61.2.42

Purpose. Pterygia are much more common nasally than temporally. Ultraviolet (UV) radiation is a major risk factor. Coroneo proposed that the nasal preference is caused by the "peripheral light focusing effect," (PLF), in which UV at an oblique angle passes through temporal cornea and is concentrated on and damages nasal limbal stem cells. This study evaluates whether the PLF is sufficient to explain the nasal preference.

Methods. Whereas Coroneo and colleagues derived the maximum PLF intensity gain (UV concentration factor) as a function of incident angle (i.e., *different* nasal limbal positions were used for different incident angles) the current analysis derived intensity gain at a *fixed* position such at the nasal corneo-limbal junction (CLJ). This provided a measure of the total PLF irradiation at this position, which was compared to total direct irradiation of nasal and temporal limbus at the corresponding positions (e.g., CLJs). In Part 1, analysis was performed like that of Coroneo, using horizontally incident UV; in Part 2, the analysis was extended to include incident rays above and below the horizontal.

Results. In both part 1 and part 2 of the study, the limbal UV irradiation of the nasal limbus from the PLF was not sufficient to explain the strong nasal location preference of pterygia.

Conclusions. The analysis calls into question the PLF explanation of nasal location preference. Other explanations of the nasal preference, and of pterygium pathogenesis, should be considered, such as temporal to nasal tear flow carrying substances such as cytokines to the nasal limbus.

Keywords: peripheral light focusing, pterygium, tears, ultraviolet light

Pterygium is a disorder of the exposed ocular surface, which involves a fleshy, fibrous, and vascular ingrowth toward the center of the cornea from the surrounding limbus.[1] As well as being unsightly, pterygia can induce significant astigmatism, glare, visual acuity and visual field loss, contact lens intolerance, ocular irritation, and dry eye.[2] Removal of a pterygium can result in scarring of the cornea. It is a common disorder, especially in equatorial regions and regions with high levels of reflected sunlight.[3,4] The prevalence is highly variable ranging from 2.8% to 33% with a pooled prevalence from 20 population-based studies of pterygia of 10.2%.[3] Although the etiology of pterygium is still subject to debate, it is thought to originate from damage to limbal stem cells, thus permitting the spread of conjunctival tissue over the cornea.[5]

The following evidence indicates that ultraviolet (UV), radiation plays a major role in the development of pterygia. The prevalence of pterygia is positively correlated with UV exposure,[6] it is increased in the regions of high UV exposure close to the equator[3] and in high UV exposure zones in Australia.[4] Although Greenland is far from the equator, the prevalence of pterygia is relatively high, presumably because of the high UV reflectance of snow.[7] The prevalence of pterygia is increased by outdoor activity, probably also due to increased UV exposure.[3] Wearing spectacles, sunglasses, and hats with brims, reduces UV ocular exposure and the prevalence of pterygia.[3] Welders, who are exposed to high levels of UV radiation, are also at increased risk of developing pterygia.[8]

In cases implicating UV exposure, nasally located pterygia are much more common than temporal. For example, Shiroma et al.[9] found that 1583 of 1692 pterygia (93.6%) had a nasal location; thus, the nasal location was 15.5 times more common than temporal. A similar asymmetry was found in other extensive studies.[10,11]

Coroneo and colleagues[12,13] proposed that this nasal preference for pterygium was due to the "peripheral light focusing effect" (PLF) of UV radiation on the nasal limbus. According to this theory, UV radiation that strikes the temporal cornea, at a large angle to the optical axis of the eye, is refracted and concentrated onto the nasal limbus and damages limbal stem cells, leading to the ingrowth of pterygia onto the cornea. The PLF does not occur in the temporal limbus due to obstruction by the nose. This theory provides an explanation for the high rate of nasally located pterygia in geographic areas where reflected UV radiation is high. However, pterygia can be associated with factors other than UV irradiation, such as high levels of dust and environ-

mental exposure to chemicals.[14,15] These cases also show a nasal preference for the location of pterygia, suggesting that factors other than the PLF may be involved in the nasal-temporal asymmetry.

It is the purpose of this article to re-examine the PLF theory as the explanation for the strong nasal location preference of pterygia. Although the analysis by Coroneo and colleagues centered mainly on the PLF aspect of UV irradiation, we include a full analysis of UV irradiation to both the nasal and temporal limbus, including PLF and the effect of direct UV irradiation. Specifically, the total nasal UV irradiation, including both the PLF and direct nasal irradiance, is studied to evaluate whether it is greater than the direct temporal irradiance.

Methods

In this study, we use ray tracing, as did Coroneo and colleagues, to study the PLF and the effect of direct irradiation at the nasal and temporal limbus. The ray-tracing simulations will be presented in two parts. In part 1, ray tracing was performed in a similar manner to the analyses of Coroneo and colleagues,[12,13] considering only horizontal incident UV. In part 2, the analysis was extended to include the full field of incident UV from all angles, including above and below the horizontal.

In our analyses, the corneal thickness and shape were the same as that used in the Kwok et al. simulations.[13] As in their study, it is assumed that most UV radiation reaching the eye is reflected from the environment rather than radiation from the sun directly striking the eye.[16,17] Simulations were performed using refractive indices of cornea and limbus 1.400, and aqueous humor 1.360, for a UV radiation at 350 nm.[18] These refractive indices agreed with the values used by Kwok et al.[13] Ray tracing was performed with a custom program written in C++ (CodeWarrior; Metrowerks, Hudson, Quebec, Canada) using the unit vector form of Snell's Law[19] with representative results checked using the ray-tracing software Zemax (Kirkland, WA, USA). General aspects of both analyses are outlined here, but specific details are added in the Results section.

For both parts 1 and 2, the irradiance at two positions on the limbus will be considered—the corneo-limbal junction, corneo-limbal junction (CLJ), and 1 mm outside the CLJ; these are shown as filled circles in Figure 1A (further explanation of Fig. 1 will be provided below). These positions give the approximate range of location for probable limbal epithelial stem cells, which are thought to be involved in the pathogenesis of pterygia.[20]

Part 1. Horizontal Incident UV

In part 1, the contribution of the PLF to UV irradiance was calculated using standard "forward ray tracing" (i.e., rays were traced from incident UV on the temporal cornea to the nasal limbus). For any incident angle, the incident ray striking a position on the limbus (e.g., the CLJ), was determined and the intensity gain for that ray calculated.

The two main differences from the analysis of Coroneo and colleagues[12,13] are the following. First, those studies calculated the maximum "intensity gain" (i.e., concentration by focusing of radiation on a "radiometer" near the limbus) as a function of incident angle; for each incident angle, the maximum intensity gain occurred at a *different* position on the radiometer. In this study, the intensity gain as a function of incident angle was calculated for a *fixed* position on the radiometer; differences between the current approach and Coroneo's are illustrated by points P (Kwok's method) and CLJ or Q (current method) in Figure 1A. Thus, a measure of total irradiance at this fixed position could be calculated by integrating intensity gain as a function of incident angle. This information cannot be derived from the study of Kwok et al.,[13] where different incident angles correspond to different positions (Ps) on the limbus. Second, measures of direct irradiance of nasal and temporal limbus were derived for comparison with the PLF irradiance (see Fig. 1B). Thus, a measure of total irradiance of nasal limbus, including both direct irradiance and the PLF, could be compared with the corresponding measure of direct temporal irradiance.

Another difference from the analysis of Kwok et al.[13] is that two measures of intensity gain were calculated in this study. "Geometric gain" corresponded to the intensity gain used by Kwok et al.[13] derived from the focusing effect of the PLF. "Overall gain" additionally included the effects of absorption and scattering in the cornea[21] and reflection from corneal surfaces derived from Fresnel's Laws of Reflectance[22] and ocular refractive indices.[18] An additional difference is that whereas the radiometer used by Kwok et al.[13] was parallel to the optic axis, in this study, the radiometer was the outer surface of the limbus, thus corresponding to the location of limbal epithelial stem cells thought to be involved in the pathogenesis of pterygia.[2,20] Our method of calculating intensity gain, which is described in Figure 2, is based on the spacing between adjacent rays on the limbus, and differs somewhat from the method of Kwok et al.[13] where the number of rays was calculated within a "bin" on their radiometer, and is, therefore, influenced by some random noise depending on the alignment of the array of ray positions and the area of the bin (i.e., whether the rays nearest the edges of a bin tend to be just inside or just outside the edges).

Part 2. Full Field Incident UV

As noted, whereas Kwok et al.[13] considered only horizontal incident rays, this analysis includes incident rays above and below the horizontal plane, and so gives a more inclusive measure of the irradiance contribution of the PLF, Figure 1C. To determine a measure of the irradiance at a fixed point on the limbus, such as the CLJ, "backward ray tracing" was used to determine the extent of rays striking this fixed point; rays were traced backward from this fixed point toward their temporal origin. Only backward rays passing through the temporal cornea contribute to the PLF; other backward rays are either totally internally reflected by temporal cornea, or strike the temporal limbus or conjunctiva. The simulations apply the "Radiance Conservation Theorem"[23] (i.e., the radiance of a uniform extended source is unaffected by passage through a lossless optical system [unless, as discussed later, the refractive index of the final medium differs from that of the incident medium]). The analysis also involves the "Nusselt Analog,"[24] which is a graphical method of deriving the irradiance of a surface from a uniform extended radiance; this method is discussed later.

Investigative Ophthalmology & Visual Science

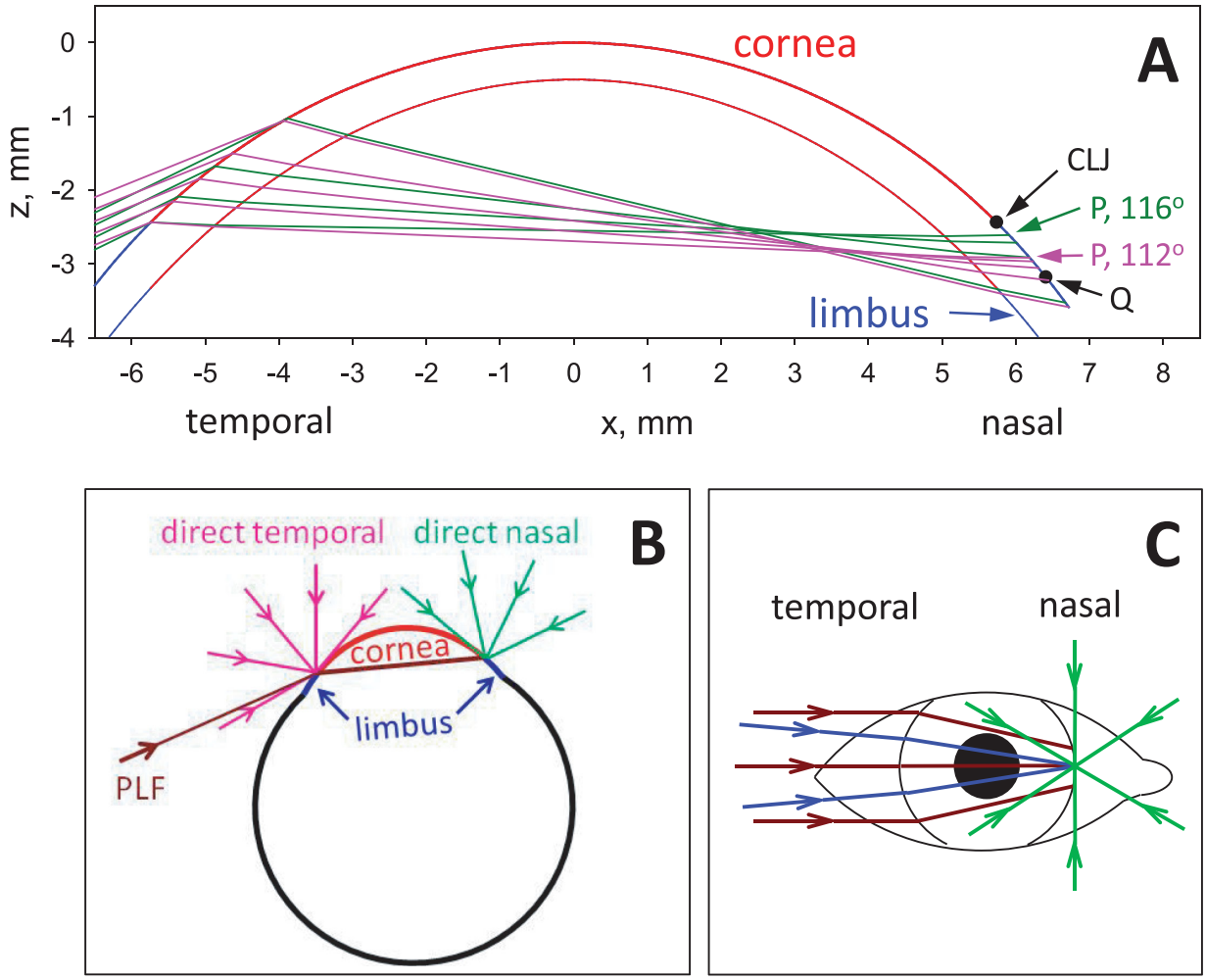

Figure 1. Illustration of major differences between the current analysis and that of Kwok et al.[13] (**A**) Forward ray tracing in the horizontal mid-plane for incident angles of 112°, pink and 116°, green. In the Kwok et al. study,[13] the maximum concentrations of UV at the two angles were derived at the different positions labeled P, 112° and P, 116°. In the current study, the concentration of UV was studied at fixed positions, the corneo-limbal junction (CLJ), and 1 mm outside the CLJ, point Q. In this way, the total irradiance at these positions can be studied by integrating contributions from different incident angles. (**B**) In addition to analyzing the PLF, the direct irradiances to the temporal and nasal limbus were also evaluated in the current study. (**C**) Whereas Kwok et al.[13] considered only horizontal incidence for analyzing the PLF, brown, the current study includes also incident rays above and below the horizontal for both the PLF, blue, and direct irradiation, green.

Results

Part 1. Horizontal Incident UV

In this part, the assumptions made are somewhat similar to those of Kwok et al.[13] based on forward ray tracing of horizontal incident rays. Some differences from their analysis have been described in the Methods section.

Figure 2A shows forward ray tracing in the horizontal mid-plane, for an incident angle of 115° to the optic axis. The thicker ray strikes the point Q, at 1 mm from the CLJ. The insets show the spacing, dh_1, between incident rays, and the spacing, dh_2, between rays striking the limbus near point Q. Thus, UV is concentrated in the horizontal direction by a factor $H = dh_1/dh_2$, which will be called the "horizontal gain" in this analysis. In the calculations, the spacing between incident rays was much smaller than in A, namely 10 nm. At this incident angle, H = 0.249. In their analysis, Kwok et al.[13] calculated the *maximum* gain for any incident angle; in this example, the maximum horizontal gain would be at position P, giving H = 1.69, a value considerably higher than at Q.

Figure 2B shows a corresponding plot for incident rays in the same vertical plane as the thicker ray in panel **A**, at the same incident angle of 115° to the optic axis. The thicker ray is the same as the thick ray in panel **A**. The insets show incident ray spacings, dv_1, and the spacing dv_2, between rays striking the limbus at 1 mm from the CLJ. Thus, UV is concentrated in the vertical direction by a factor $V = dv_1/dv_2$, which will be called the "vertical gain." In the calculations, the spacing between incident rays was 10 nm. At this incident angle, V = 4.63. Thus, a "geometric gain," G, corresponding to the intensity gain of Kwok et al.,[13] is given by the product of horizontal and vertical gains (i.e., G = HV = 1.15). In the type of analysis used by Kwok et al.,[13] the maximum geometric gain at point P is G = 5.19 and, so, at this incident angle, is considerably higher than the intensity gain at the fixed point, Q, used in this analysis.

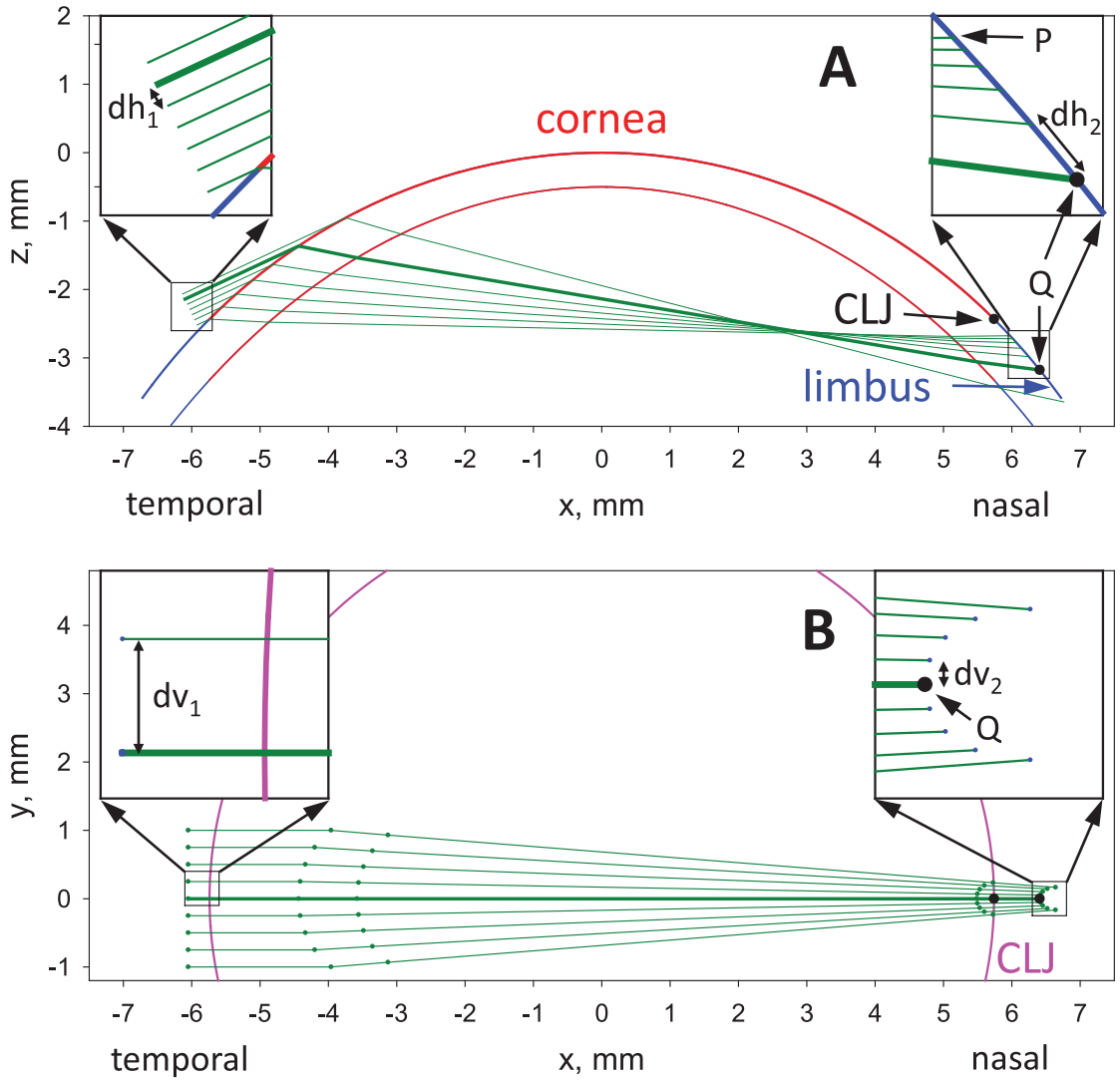

Figure 2. Forward ray tracing for an incident angle of 115° to the optic axis, illustrating the derivation of horizontal and vertical gain. (A) Ray tracing in the horizontal mid plane. Filled circles show the two nasal positions in this study – the CLJ and 1 mm outside the CLJ, point Q. The thicker ray striking at Q, 1 mm outside the nasal CLJ, is the same as the thicker ray in panel B. Insets show enlargements of temporal and nasal rays, showing definitions of dh_1 and dh_2 at Q, 1 mm outside the CLJ, used in the calculation of "horizontal gain," dh_1/dh_2 (in practice, dh_1 was much smaller, 10 nm). (B) Ray tracing projected on a vertical plane parallel to the optic axis. Incident rays were in a vertical plane at an incident angle of 115° to the optic axis. The thicker ray is the same as the thicker ray in panel A. Small dots show intersections of rays with the corneal and limbal surfaces. Insets show enlargements of temporal and nasal rays showing definitions of dv_1 and dv_2, used in the calculation of "vertical gain," dv_1/dv_2 (in practice, dv_1 was much smaller, 10 nm).

The red curves in Figure 3 show geometric gain as a function of incident angle at the two studied points on the nasal limbus; panel A is for the CLJ and panel B is for 1 mm outside the CLJ. The open circle in panel B gives the value of geometric gain at 1 mm outside the CLJ for incident angle 115°, derived from the ray tracing of Figure 2. It is seen that, at 1 mm outside the CLJ, the geometric gain can reach a high value of around 22, in agreement with similar values in Kwok et al.[13] However, this high gain occurs over a very limited range of incident angle. A measure of total irradiation at the two positions on the nasal limbus can be derived by integrating the geometric gain as a function of angle (i.e., the area under the red curves); this will be called the "integrated PLF geometric gain." At the CLJ, panel A, the integrated PLF geometric gain is 11.5°, whereas at 1 mm outside the CLJ, panel B, it is 22.7°. It will be argued that these PLF contributions to irradiance are relatively small compared to the direct irradiances of temporal and nasal limbus, which occur over much wider angles that the PLF angle range in Figure 3.

The irradiation of the nasal limbus by the PLF is affected by a "transmission factor," including the effects of absorption and scattering in the cornea and reflection at corneal surfaces. To derive the effect of corneal absorption and scattering, we used values for 350 nm derived from table 4 of van de Kraats and van Norren[21] and used the Beer-Lambert Law to calculate the effect of corneal path length on attenuation.[25] The wavelength of 350 nm in the UVA region of the spectrum was chosen rather than a UVB wavelength, such as 300 nm, because the PLF irradiation of the limbus would be much less at 300 nm due to greater absorption and scattering by transmission through the cornea.[21] For normal incidence, the optical density of the cornea increases from

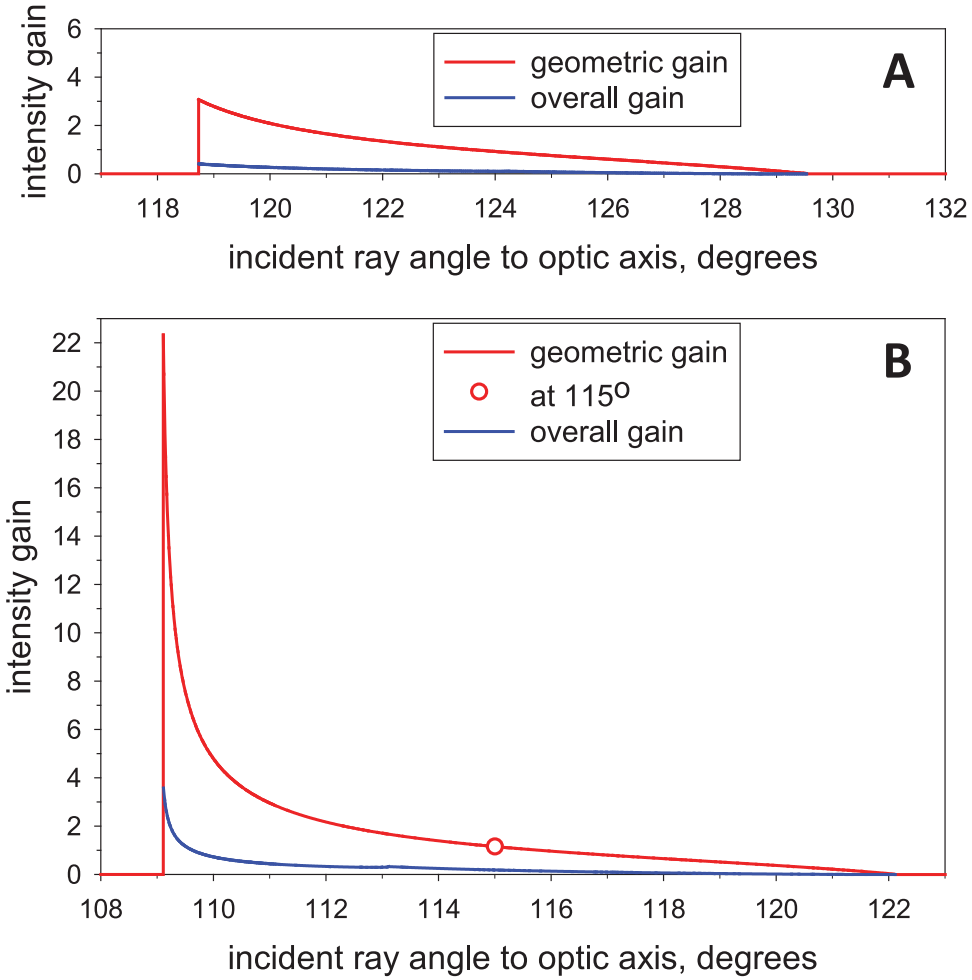

Figure 3. Intensity gain as a function of the incident angle to the optic axis. Geometric gain (red) is the product of horizontal and vertical gain (see Fig. 2). Overall gain (blue) includes the effect of reflection from corneal surfaces and absorption and scattering in the cornea. (A) At the nasal CLJ. (B) At 1 mm outside the CLJ. Open circle is the value of geometric gain at 115° derived from Figure 2.

0.237 at 350 nm to 1.139 at 300 nm[21], so the transmittance is reduced from 58% at 350 nm to 7.3% at 300 nm; given that the PLF involves double passage through the cornea at an oblique angle, its contribution at 300 nm would be much less than given in this analysis using 350 nm. To derive the effect of corneal surface reflectance, we applied Fresnel's Laws of Reflectance[22] using refractive index values of cornea and aqueous humor[18]; calculations included the effect of increased irradiance from reflection at the outer nasal limbal surface, and were made separately for "s" and "p" polarizations of incident radiation[22] with the transmission factors for the two polarizations being averaged. For each incident angle, an "overall gain" was calculated as the product of transmission factor and geometric gain and is given by the blue curves in Figure 3. Integrals of overall gain as a function of incident angle were 1.34° at the CLJ and 3.41° at 1 mm outside the CLJ; these will be called the "integrated PLF overall gain."

To evaluate the overall contribution of the PLF to nasal irradiation, it is important to consider the direct irradiation of the limbus, as illustrated in Figure 4 for the nasal and temporal CLJ. The shape of the cornea and limbus are again given by the parameters of Kwok et al.[13] The angle Kappa between the visual and optic axis is assumed to be 5°.[26] The nose restricts the nasal visual field to within about 63° of the visual axis[28]; whereas this angle corresponds to rays striking the pupil, a similar angle may reasonably be assumed to apply at the nasal limbus (see Fig. 4). Thus, Figure 4B indicates that the total horizontal angle irradiating the nasal CLJ is about 113° depending on the projection of the nose. At the temporal CLJ, there is some obstruction of irradiation by the lateral canthus, which may restrict the total angle of irradiation to about 160° according to Figure 2b of Atchison et al.[27]; whereas this value is uncertain because it is derived from just a single example, it is probably about a lower limit because a smaller value would cause considerable interference with the PLF (compare Fig. 4 with Fig. 2A). At 1 mm outside the CLJ, the corresponding total nasal and temporal irradiation angles are estimated to be 107° and 157°, respectively.

To derive a measure of total direct nasal and temporal irradiation, corresponding to the integrated geometric gain of the PLF, integration can be made over the exposed angles, θ, weighted by the cos(θ) dependence of irradiance on illumination angle.[23] It was assumed that the radiance of the nose was 15% of the full field direct radiance, corresponding to the reflectance of skin in the UV.[29] Note that people with darker skin probably have reduced UV reflectance from the

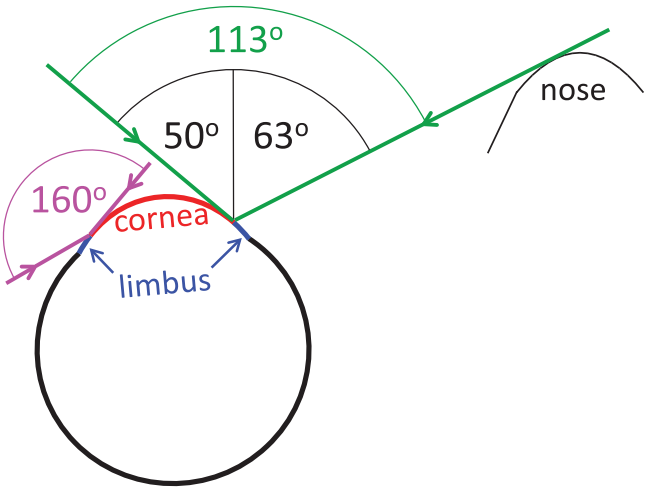

Figure 4. Comparison of direct irradiation of the temporal and nasal corneo-limbal junctions (CLJ), in the horizontal mid plane. At the temporal CLJ, there is only a slight obstruction near the lateral canthus[27] allowing an angle of about 160° of irradiation. At the nasal CLJ, the nose restricts irradiation to about 63° from the visual axis, allowing an angle of irradiation of about 113°. The corneal shape is based on Kwok et al., 2004.[13] The angle kappa between the visual and optic axes is assumed to be 5°.[26]

nose; this would reduce overall irradiance of nasal limbus, thus reducing the effect of the PLF. Thus, the measure of nasal direct irradiance (corresponding to the "integrated PLF geometric gain" described above) becomes:

$$N_g = \int_{-90}^{23} \cos(\theta)\, d\theta + 0.15 \int_{23}^{90} \cos(\theta)\, d\theta \qquad (1)$$

where angles are measured in degrees in a clockwise direction from the normal to the CLJ, and the number 23 corresponds to 113° to 90° (see Fig. 4); N_g will be called the "integrated direct nasal geometric gain" and was evaluated to be 84.9°. A corresponding integration was made at the temporal CLJ, assuming that the lateral canthus also reflects 15% of incident light,[29] giving a value of 111.7°; this is greater than the total value for the nasal CLJ, given by the sum of direct nasal irradiance and PLF, namely, 84.9° + 11.5° = 96.4°. Corresponding integrations were made for 1 mm outside the nasal CLJ, and for the corresponding temporal CLJ position, and results will be summarized in Figure 5.

Direct irradiation of cells just below the surface of the limbus (such as limbal epithelial stem cells) is attenuated by reflection at the limbal surface. Thus, a measure of overall direct irradiance at the nasal CLJ is given by modifying Equation 1 to:

$$N_o = \int_{-90}^{23} t(\theta) \cos(\theta)\, d\theta + 0.15 \int_{23}^{90} t(\theta) \cos(\theta)\, d\theta \qquad (2)$$

where $t(\theta)$ is the transmittance of the limbal surface given by Fresnel's Laws of Reflectance[22]; and N_o will be called the "integrated direct nasal overall gain." Corresponding integrations were made for 1 mm outside the nasal CLJ, and for the corresponding temporal CLJ positions.

A summary of the conclusions of part 1, Horizontal Incident UV, is given in Figure 5, which compares total UV irradiance at temporal (T), and nasal (N), limbus. Integrated gain, a measure of irradiance, is given for both geometric gain and overall gain, as well as at both the CLJ and 1 mm outside the CLJ. In all four comparisons, the total nasal irradiance, which is the sum of direct irradiance and the PLF, is less than the total temporal irradiance. (As noted previously, the PLF at 1 mm outside the CLJ would be further attenuated by an unknown back scattering by the limbal stroma, thus further reducing the total nasal irradiation at this location.) Because anatomic variations, such as the shape of the nose and scleral topography, can affect the calculation of direct nasal irradiation, the rightmost column in Figure 5, labeled N*, shows the effect on "overall" irradiance of increasing the total nasal irradiation angle of 107° by 15° to 122° (e.g., due to shorter nose and flatter sclera); whereas the total nasal irradiance is increased, it is still seen to be less than the total temporal irradiance. This analysis, therefore, indicates that the PLF probably does not explain the strong nasal preference of pterygia.

Part 2. Full Field Incident UV

In this part of the results, a more exact analysis of the PLF contribution to irradiance includes incident UV from above and below the horizontal, in addition to the horizontal incidence considered by Kwok et al.[13] and in part 1. This "full field" analysis was applied to both the PLF and direct irradiation. The principle of the analysis is to consider a point on the limbus, such as the CLJ, and analyze the solid angle of irradiation converging on that point. The eye will be assumed to view a uniform radiance, L_1, in the visual field. According to the Radiance Conservation Theorem, the radiance observed through a lossless optical system is:

$$L_2 = (n_2/n_1)^2 L_1 \qquad (3)$$

where n_1 and n_2 are the refractive indices of the incident medium (air) and final medium (limbus).[23] The final irradiance would be modified by reflection at corneal surfaces, and absorption and scattering in the cornea; as noted in part 1, the overall effect of these factors is attenuation of final irradiance. The analysis will be performed first for the lossless system of Equation 3, and this attenuation will be considered later.

The irradiance, dE, at a point on a surface from an element of solid angle, $d\Omega$, of a uniform radiance, L, is given by:

$$dE = L\cos(\theta) d\Omega \qquad (4)$$

where θ is the angle of incidence on the surface.[24] Thus, the total irradiance, E, at the point is given by integration over solid angle:

$$E = L \int \cos(\theta) \mathrm{d}\Omega \qquad (5)$$

where the integral is performed over all directions of irradiation. Thus, derivation of irradiance at the point depends on determining the total solid angle irradiating that point, together with the variation of the angle of incidence within that solid angle.

"Backward ray tracing" was used to derive the total solid angle irradiating the limbus from the PLF, and is illustrated in Figure 6. Backward rays were considered "valid" if they struck the corneal surface, rather than the limbus or conjunc-

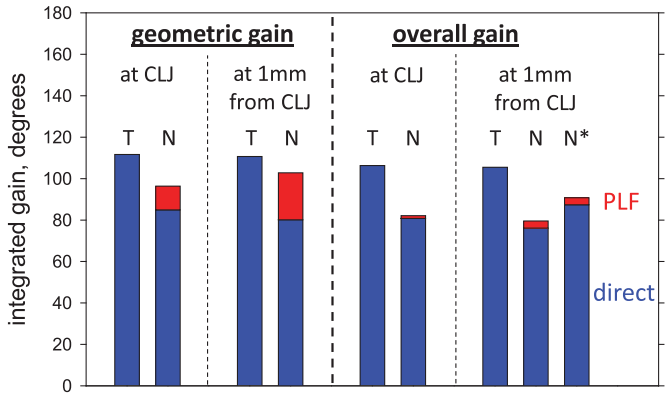

Figure 5. Measures of total UV irradiance at temporal (T) and nasal (N) limbus, including PLF (red) on the nasal limbus and direct irradiance (blue) on both nasal and temporal limbus. The rightmost bar, N*, corresponds to an assumed increase in direct nasal irradiation of 15° (e.g., due to a shorter nose). "Integrated gain" is, for the PLF, the integral of gain (as in Fig. 3) as a function of incident angle, and, for direct irradiance, Equations 1 and 2.

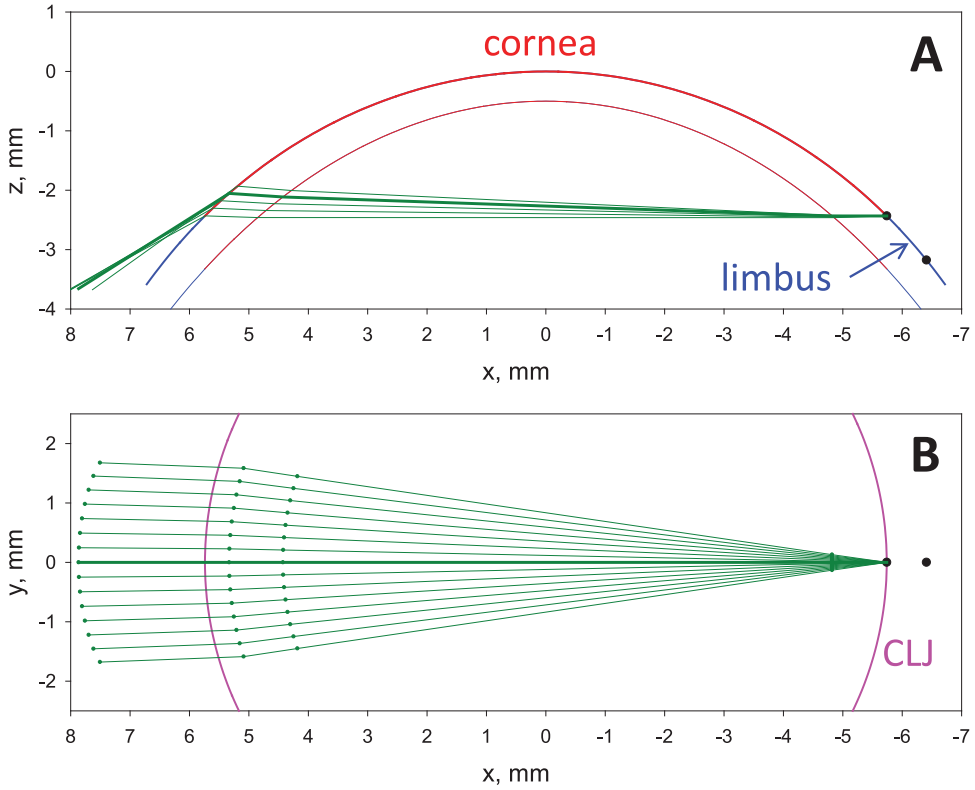

Figure 6. Backward ray tracing from a point on the corneo-limbal junction (CLJ) in the horizontal mid-plane. Black circles show the CLJ and 1 mm outside the CLJ. (**A**) Rays in the horizontal mid-plane. The thicker ray is the same as the thicker ray in panel **B**. (**B**) Rays lying in a vertical plane in the nasal cornea before striking the corneo-limbal junction (in other regions, the rays are no longer in a vertical plane). The thicker ray is the same as the thicker ray in panel **A**. Small dots show intersections of rays with the corneal surfaces.

tiva, and emerged from the cornea, rather than being totally internally reflected. Thus, the integral in Equation 5 could be evaluated for all valid backward rays for a matrix of horizontal and vertical angles.

Two methods were used to evaluate the integral of Equation 5 for the PLF, and, hence, to derive the irradiance, E, of the limbus for a given radiance, L. Both methods produced the same results, helping to confirm the validity of the calculations. One method is to evaluate the integral numerically, which can be done using the x, y, z coordinate system of Figure 6. A second method is to use a graphical procedure called the Nusselt Analog,[24] which is illustrated in Figure 7. The results of this method are presented here because they provide a better insight into the analysis, and also allow comparison with the irradiance from direct irradiation of nasal and temporal limbus.

To illustrate the Nusselt Analog, in Figure 7A, a small element of solid angle, $d\Omega$, subtended at a point P on a

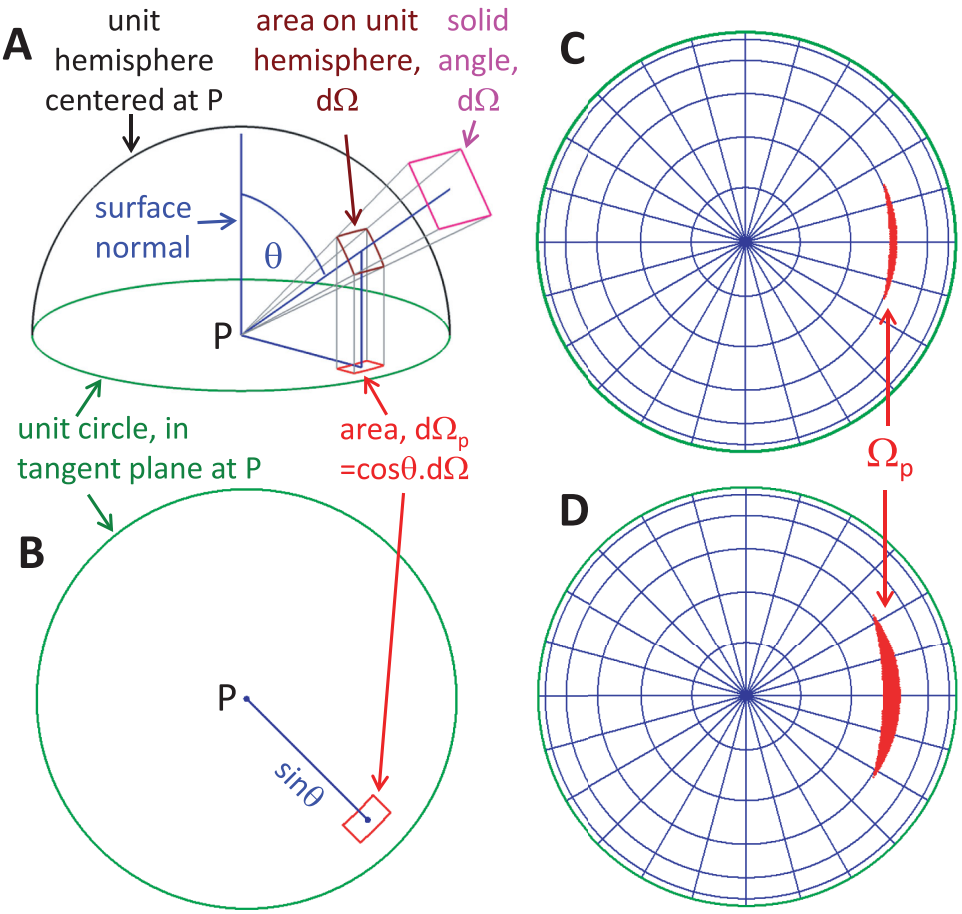

Figure 7. Application of the Nusselt Analog in analyzing irradiance from the PLF. (**A**) Illustration of the Nusselt Analog showing the derivation of "projected solid angle," $d\Omega_p$, a measure of irradiance at a point P on a surface, from a small uniform source of solid angle $d\Omega$ at an illumination angle θ. The source is a square (pink) at right angles to the line of sight. See text for details, **B**. Plot of the projected solid angle in the unit circle—the irradiance at P is proportional to $d\Omega_p$. (**C**). Unit circle showing the total projected solid angle, Ω_p, from the PLF, irradiating a point at the corneo-limbal junction (CLJ). Blue lines indicate polar and azimuthal angles at 15° intervals. (**D**) Total projected solid angle, as in panel **C**, but for a point 1 mm outside the CLJ.

surface, is first projected down to an area, $d\Omega$, on a unit sphere centered at P, and then is projected orthographically onto the unit circle in the tangent plane at P, forming a "projected solid angle," $d\Omega_p$.[24] The element, $d\Omega_p$, is shown in the unit circle in Figure 7B and is at a distance $\sin(\theta)$ from P. The area, $d\Omega_p$, is equal to $\cos(\theta)d\Omega$ so Equation 5 may be written

$$E = L\int d\Omega_p = L\Omega_p \quad (6)$$

where Ω_p is the total projected solid angle. Thus the irradiance, E, at point P, is proportional to Ω_p.

To apply the Nusselt Analog to determine the total projected solid angle from the PLF, the coordinates used in Figure 7 were first transformed to the coordinates of Figure 6 by rotation about the vertical axis through an angle corresponding to the slope of the point on the limbus (CLJ or 1 mm outside the CLJ); backward ray tracing was then used to test whether the ray contributed to the PLF. Figures 7C and 7D show the projected solid angles for the PLF derived for the same assumptions of refractive indices and ocular surface shape as in part 1; Figures 7C and 7D correspond to the CLJ and 1 mm outside the CLJ, respectively. Test points in the unit circle were spaced at intervals of 0.005 in both the horizontal and vertical directions, and the area of Ω_p was calculated by multiplying the number of valid test points by 0.005^2. The corresponding areas, Ω_p, were 0.0124 at the CLJ, Figure 7C, and 0.0428 at 1 mm outside the CLJ, Figure 7D. It should be noted that (ignoring transmission losses), compared to the radiance from the environment, the radiance at the limbus is increased by a factor of the square of limbal refractive index according to Equation 3. Correcting for this factor, the corresponding areas, Ω_p, were 0.0243 at the CLJ, and 0.0838 at 1 mm outside the CLJ.

Application of the Nusselt Analog in analyzing the *direct* irradiance of the limbus is illustrated in Figure 8. The principle is to estimate the "visual field" visible from the surface of the limbus, analogous to the visual field determined by perimetry. The dotted curve in Figure 8A is the perimetric visual field for a 10/1000 target[28]; this target size was chosen because larger targets made little difference to the visual field, whereas smaller targets gave considerably smaller visual fields because of limitations in visual sensitivity. The center of Figure 8A corresponds to the visual axis. The solid red curve gives the assumed exposed solid angle at the pupil position and has been limited to a maximum eccentricity of 90°. Figure 8A has been replotted in Figure 8B on

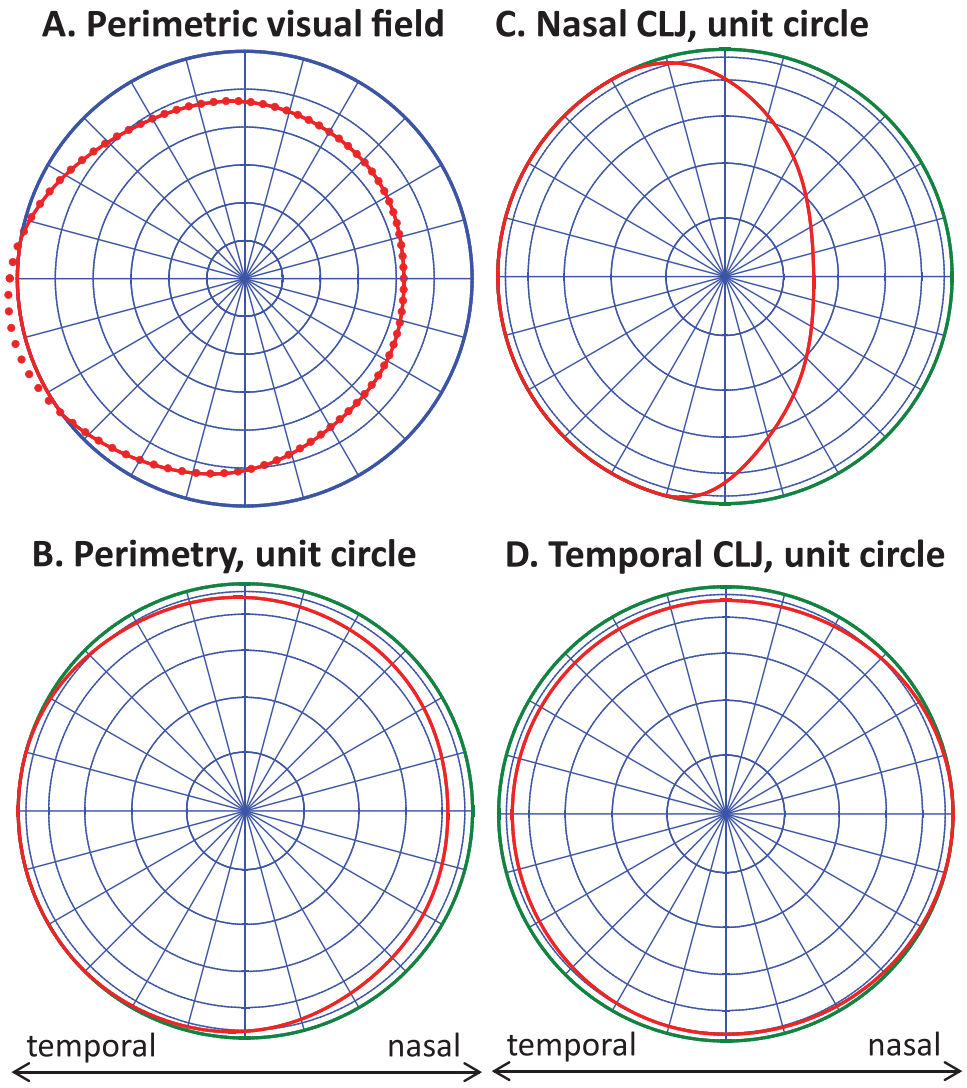

Figure 8. Application of the Nusselt Analog in analyzing direct irradiance of nasal and temporal CLJ. Blue lines indicate polar and azimuthal angles at 15° intervals. (**A**) Dotted curve is visual field of left eye for 10 of 1000 target. Solid red curve is the assumed exposed solid angle at the pupil position. (**B**) Projected solid angle in the unit circle derived from the exposed solid angle in A using the Nusselt Analog (see Fig. 7). (**C**) Projected solid angle irradiating nasal CLJ which is assumed to slope at 40° compared to central cornea. (**D**) Projected solid angle at temporal CLJ. See text for details.

the unit circle of the Nusselt Analog; thus, the area within this curve is the projected solid angle, $\Omega_p = 2.840$, of the visual field.

To evaluate the direct irradiance at the nasal limbus, Figure 8C shows the unit circle plot for the visual field visible from the nasal CLJ. This was obtained after rotating the unit sphere used to determine Figure 8B through an angle of 40° about the vertical axis—this angle corresponds to the slope at the surface of the CLJ compared to the central cornea. It is seen that the projected solid angle, $\Omega_p = 2.055$, is reduced compared to the perimetric visual field in Figure 4B, due to increased obstruction by the nose on the right hand side. Figure 8D is an estimate of the unit circle plot for the visual field visible from the temporal CLJ. Because the perimetric visual field does not provide information about blocking of radiation by the lateral canthus, it was assumed that the lateral canthus acted as a vertical edge at 70° from the normal—cf. Figure 4. In a similar way, the brow and the cheek were simulated by horizontal edges at 70° above and 76° below the horizontal, respectively; these angles were derived from the extent of the vertical meridian of the perimetric visual field in Figure 8A. It is seen that the projected solid angle, $\Omega_p = 2.909$, is slightly greater than for the perimetric visual field in Figure 8B, and considerably greater than for the nasal CLJ in Figure 8C. At 1 mm outside the CLJ, corresponding values of direct nasal and temporal projected solid angles were calculated to be 1.901 and 2.880, respectively.

Figure 9 summarizes the total irradiation at the nasal and temporal limbus based on the Nusselt Analog analysis of full field irradiation illustrated in Figures 7 and 8. As indicated in Figure 5, including the effects of reflection from corneal surfaces and of absorption and scattering in the cornea, would have reduced the relative contribution of the PLF even further (compare "overall gain" with "geometric gain" in Fig. 5). These results support the conclusion of Figure 5 in part 1 (horizontal incidence) that the PLF probably does not explain the strong nasal preference for pterygia.

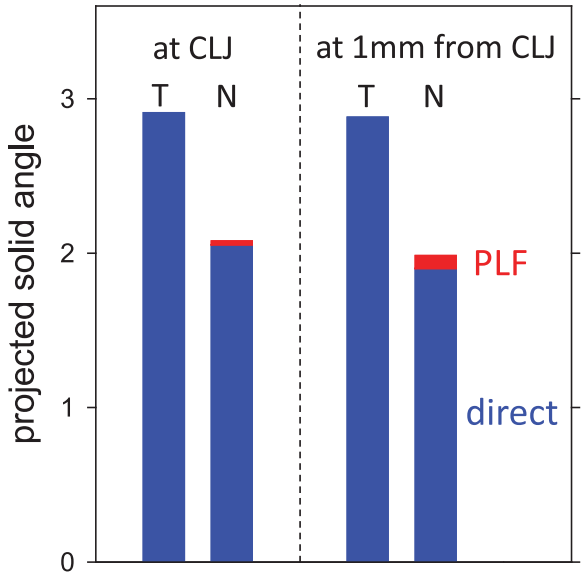

Figure 9. Measures of total UV radiation at temporal (T) and nasal (N) limbus, including PLF, red, on the nasal limbus and full field direct radiation, blue, on both nasal and temporal limbus. "Projected solid angle" is derived from the Nusselt Analog analysis of Figures 7 and 8. The projected solid angle for the PLF has been corrected for the limbal refractive index according to Equation 3.

Discussion

The pathogenesis of pterygium is poorly understood.[2] A remarkable fact, which needs explanation by any theory, is the strong nasal location preference.[9–11] Coroneo and colleagues have proposed that the nasal preference is due to the PLF.[12,13] Our simulations are consistent with theirs in showing that UV can be concentrated (geometric gain) by a factor of about 20 (Fig. 3B). However, this gain occurs over a narrow range of incident angles, Figure 3, whereas direct irradiation of nasal and temporal limbus occurs over a much wider range of angles. Direct nasal irradiation is restricted by the nose, with the result that total nasal UV irradiance was predicted to be less than temporal irradiance (Fig. 5). A more extensive analysis involving incident rays above and below the horizontal gave the same result (Fig. 9). Our analysis does not seem consistent with the proposal that the nasal location preference of pterygia is due to the PLF.

A limitation of the current study is that, relative to the PLF, direct irradiation of stem cells in the limbus may be attenuated, by an unknown amount, by absorption in melanin. For example, Higa et al.[30] observed melanin granules in the apex of putative limbal epithelial stem cells. According to the data for 1 mm outside the CLJ on the right of Figure 9, if direct irradiation of nasal and temporal limbus was attenuated by melanin by a factor 11.7 without change to the PLF irradiation, total irradiation of nasal limbus would equal that of temporal limbus; this factor would need to be increased to take account of any back scattering of the PLF in the nasal limbus, together with reflection from corneal surface and scattering and absorption in the cornea. Greater attenuation of direct irradiation would cause total nasal irradiation to exceed temporal. However, it may be noted that the PLF could also be attenuated by melanocytes located beneath limbal epithelial stem cells, thus reducing the irradiance of the PLF compared to direct irradiance.[31]

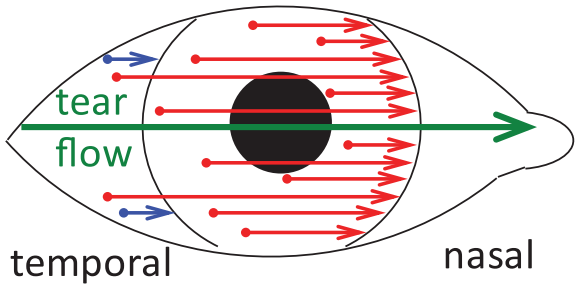

Figure 10. A possible alternative explanation of the nasal location preference of pterygia in terms of the temporal to nasal tear flow (TNTF). Dots at the right end of red and blue arrows represent substances entering the tear film (e.g., from UV damage to the underlying cornea and conjunctiva). Arrows show how these substances are carried nasally by the TNTF. Red arrows show that there is more accumulation of these substances at the nasal limbus than at the temporal limbus (blue arrows) explaining the nasal preference for pterygia.

It is important to consider other explanations for the strong nasal preference of pterygia. The following nasal-temporal asymmetries of the ocular surface could be considered:

1. The main lacrimal gland has a temporal location.
2. The lacrimal drainage system has a nasal location.
3. The density of goblet cells is considerably greater nasally than temporally.[32]
4. The plica semilunaris is located nasally with no corresponding temporal tissue.
5. The caruncle is located nasally with no corresponding temporal tissue.

The first two asymmetries, temporal lacrimal gland and nasal drainage location, imply that there is a general temporal to nasal tear flow (TNTF). Elliot[33] proposed that the TNTF was the cause of the nasal location preference of pterygia, noting that "The fact that the stream of tears, carrying its freight of dust to the lachrymal passages, always sets inwards to reach the canaliculi, naturally ordains that the greatest stress of irritation shall fall on that portion of the conjunctiva which lies internal to the cornea. It is for this reason that … pterygia are more often found on the inner than on the outer side of the eye." In addition to the possible effect of dust, it is postulated that UV exposure to the cornea and conjunctiva releases substances, such as cytokines, into the tear film, which are a causative factor for pterygia. As illustrated in Figure 10, the TNTF will cause the concentration of these substances to be higher at the nasal than at the temporal limbus, due to accumulation as the tears flow over the cornea.

It is not obvious how the last three of the five listed nasal-temporal asymmetries, high nasal goblet cell density and the nasal location of the plica semilunaris and caruncle, could give rise to the nasal preference for pterygia. Rather, it is suggested that these three asymmetries may be a consequence of the same TNTF. which Elliot[33] proposed could explain the nasal preference for pterygia. It should be considered whether these three asymmetries help to protect nasal conjunctiva from the accumulation of pathogens, antigens. and debris caused by the TNTF.

If Elliot's theory[33] of the nasal preference of pterygia is correct, this should have important implications for understanding ocular surface disorders. Applying Elliot's theory

to the effect of UV radiation, pterygia would arise from an "indirect" mechanism whereby the cornea and conjunctiva are damaged locally by UV radiation, but then release substances into the tear film. which are carried by TNTF to the nasal limbus. In other ocular surface disorders, UV radiation may act directly on the conjunctiva or cornea—this could be described as a "direct" mechanism and would be expected to cause less nasal-temporal asymmetry. An example involving a large contribution from the "direct" mechanism might be pinguecula; Norn[7] reports a more equal nasal-temporal balance in pingueculae with 607 of 958 (63.4%) being nasal in Greenland but only 303 of 689 (44.0%) being nasal in Copenhagen. Mimura et al.[34] reported 524 of 1047 (50.0%) nasal pingueculae.

Elliot's TNTF theory[33] should, therefore, be considered as an alternative explanation of the strong nasal location preference of pterygia. To evaluate his theory, it would be important to study release of substances into the tear film by UV exposure, and their possible role in the pathogenesis of pterygia. For example, Holopainen et al.[35] reported increased levels of MMP-2, MMP-9, IL-1β, and IL-8 in the tear film of patients with climatic droplet keratopathy, a disorder associated with UV exposure; UVB caused secretion of the same substances from human corneal epithelial cells. MMP-2, MMP-9, IL-1β, and IL-8 are also involved in the pathogenesis of pterygia[36] as might be predicted from Elliot's theory.[33] It should be noted that this agreement is only suggestive rather than conclusive, so further attempts to explain the strong nasal preference should be encouraged.

Coroneo[37] indicated the value of side protection in sun glasses in blocking the PLF and, thus, protecting against nasal pterygia. If the PLF is not the main cause of the nasal preference of pterygia, this advice may be less important, but should still be considered because blocking direct irradiation with sun glasses without side protection would increase the relative contribution of the PLF.

In conclusion, the origin of the strong nasal preference of pterygia deserves further study. A series of separate but correlated experiments needs to be performed to quantify the contributing effects of the nasal bias co-factors discussed. Other explanations, such as Elliot's TNTF theory,[33] should be evaluated, with experiments performed to study abnormalities in tear composition in patients with pterygia, and their possible role in pterygium pathogenesis. Such studies would be important not only in understanding the origin of the nasal preference, but also, more generally, in the analysis of pathogenesis of pterygia.

Acknowledgments

The authors thank Richard J. Braun, PhD, and Jan P.G. Bergmanson, PhD, for their expert advice on our study.

Supported by an unrestricted grant from Allergan, Dublin, Ireland (PEK-S).

Disclosure: **P.E. King-Smith,** None; **T.F. Mauger,** None; **C.G. Begley,** None; **P. Tankam,** None

References

1. Chui J, Di Girolamo N, Wakefield D, Coroneo MT. The pathogenesis of pterygium: Current concepts and their therapeutic implications. *Ocul Surf*. 2008;6:24–43.
2. Coroneo MT, Chui J. Pterygium. In: Holland EJ, Mannis MJ, Lee WB, eds. *Ocular surface disease: cornea, conjunctiva and tear film*. London: Elsevier/Saunders; 2013:125–144.
3. Liu L, Wu J, Geng J, Yuan Z, Huang D. Geographical prevalence and risk factors for pterygium: A systematic review and meta-analysis. *BMJ Open*. 2013;3:e003787.
4. Moran DJ, Hollows FC. Pterygium and ultraviolet radiation: A positive correlation. *Br J Ophthalmol*. 1984;68:343–346.
5. Di Girolamo N. Moving epithelia: tracking the fate of mammalian limbal epithelial cells. *Prog Retin Eye Res*. 2015;48:203–225.
6. Threlfall TJ, English DR. Sun exposure and pterygium of the eye: A dose-response curve. *Am J Ophthalmol*. 1999;128:280–287.
7. Norn MS. Prevalence of pinguecula in Greenland and in Copenhagen, and its relation to pterygium and speroid degeneration. *Acta Ophthalmologica*. 1979;57:96–105.
8. Karai I, Horiguchi S. Pterygium in welders. *Br J Ophthalmol*. 1984;68:347–349.
9. Shiroma H, Higa A, Sawagachi S, et al. Prevalence and risk factors of pterygium in a southwestern island of Japan: The Kumejima Study. *Am J Ophthalmol*. 2009;148:766–771.
10. Wu K, He M, Xu J, Li S. Pterygium in aged population in Doumen County, China. *Yan ke xue bao*. 2002;18:181–184.
11. Youngson RM. Pterygium in Israel. *Am J Ophthalmol*. 1972;74:954–959.
12. Coroneo MT, Muller-Stolzenburg NW, Ho A. Peripheral light focusing by the anterior eye and the ophthalmohelioses. *Ophthalmic Surg*. 1991;22:705–711.
13. Kwok LS, Daszynski DC, Kuznetsov VA, Pham T, Ho A, Coroneo MT. Peripheral light focusing as a potential mechanism for phakic dysphotopsia and lens phototoxicity. *Ophthal Physiol Opt*. 2004;24:119–129.
14. Detels R, Dhir SP. Pterygium: A geographical study. *Arch Ophthalmol*. 1967;78:485–491.
15. Lin W, Wang S-L, Wu H-J, et al. Associations between arsenic in drinking water and pterygium in southwestern Taiwan. *Environ Health Perspect*. 2008;116:952–955.
16. Sliney DH. Physical factors in cataractogenesis: Ambient ultraviolet radiation and temperature. *Invest Ophthalmol Vis Sci*. 1986;27:781–790.
17. Walsh JE, Bergmanson JPG. Ocular visible light and ultraviolet radiation transmittance. *Clinical Ocular Anatomy and Physiology*. 26th ed. Houston, TX: Texas Eye Research and Technology Center; 2019:70–75.
18. Atchison DA, Smith G. Chromatic dispersions of the ocular media of human eyes. *J Opt Soc Am A*. 2005;22:29–37.
19. Goodman DS. Geometric optics. In: Bass M , ed. *Handbook of Optics*. New York, NY: McGraw-Hill; 2010:1–24.
20. Shortt AJ, Secker GA, Munro PM, Khaw PT, Tuft SJ, Daniels JT. Characterization of the limbal epithelial stem cell niche: novel imaging techniques permit in vivo observation and targeted biopsy of limbal epithelial stem cells. *Stem Cells*. 2007;25:1402–1409.
21. van de Kraats J, van Norren D. Optical density of the aging human ocular media in the visible and the UV. *J Opt Soc Am A*. 2007;24:1842–1857.
22. Born M, Wolf E. *Principles of Optics*. Oxford: Pergamon; 2013:38.
23. Zalewski EF. Radiometry and photometry. In: Bass M , ed. *Handbook of Optics*. New York, NY: McGraw-Hill; 2010:34–12.
24. Borel CC, Siegfried AW, Powers BJ. The radiosity method in optical remote sensing of structured 3-D surfaces. *Remote Sens Environ*. 1991;36:13–44.
25. Lakowicz JR. *Principles of Fluorescence Spectroscopy*. 3rd ed. New York, NY: Springer; 2006:58–59.

26. Hashemi H, KhabasKhoob M, Yasdani K, Mehravaran S, Jafarzadehpur E, Fotouhi A. Distribution of angle Kappa measurements with Orbscan II in a population-based survey. *J Refract Surg*. 2010;26:966–971.
27. Atchison DA, Jones CE, Schmid KL, et al. Eye shape in emmetropia and myopia. *Invest Ophthalmol Vis Sci*. 2004;45:3380–3386.
28. Traquair HM. *An Introduction to Clinical Perimetry*. London: Mosby; 1938:4.
29. Nielsen KP, Zhao L, Juzenas P, Stamnes JJ, Stamnes K, Moan J. Reflection spectra of pigmented and nonpigmented skin in the UV spectral region. *Photochem Photobiol*. 2004;80:450–455.
30. Higa K, Shimmura S, Miyashita H, Shimazaki J, Tsubota K. Melanocytes in the corneal limbus interact with K19-positive basal epithelial cells. *Exp Eye Res*. 2005;81:218–223.
31. Pinnamaneni N, Funderburgh JL. Concise review: Stem cells in the corneal stroma. *Stem Cells*. 2012;30:1059–1063.
32. Kessing SV. Mucous gland system of the conjunctiva: A quantitative normal anatomical study. *Acta Ophthalmol (Copenh)*. 1968;95 (suppl.):1–133.
33. Elliot RH. *Tropical Ophthalmology*. London, England: Oxford Medical Publications; 1920.
34. Mimura T, Usui T, Obata H, et al. Severity and determinants of pinguecula in hospital-based population. *Eye Contact Lens*. 2011;37:31–35.
35. Holopainen JM, Robciuc A, Cafaro TA, et al. Pro-inflammatory cytokines and gelatinases in climatic droplet keratopathy. *Invest Ophthalmol Vis Sci*. 2012;53:3527–3535.
36. Zhou W-P, Zhu Y-F, Zhang B, Qui W-Y, Yao Y-F. The role of ultraviolet radiation in the pathogenesis of pterygia. *Mol Med Rep*. 2016;14:3–15.
37. Coroneo MT. Pterygium as an early indicator of ultraviolet insolation: A hypothesis. *Br J Ophthalmol*. 1993;77:734–739.

Investigative Ophthalmology & Visual Science